

Bioengineered NRF2-siRNA is effective to interfere with NRF2 pathways and improve chemosensitivity of human cancer cells

Peng-Cheng Li, Mei-Juan Tu, Pui Yan Ho, Joseph L. Jilek, Zhijian Duan, Qian-Yu Zhang,
Ai-Xi Yu, Ai-Ming Yu

Department of Orthopedics, Zhongnan Hospital of Wuhan University, Wuhan, Hubei 430071,
China (P.-C. L., A.-X. Y.); Department of Biochemistry & Molecular Medicine,
Comprehensive Cancer Center, UC Davis School of Medicine, Sacramento, CA 95817, USA
(P.-C. L., M.-J. T., P.Y. H., J.L. J., Z. D., Q.-Y.Z., A.-M. Y.)

Running title: Bioengineered NRF2-siRNA enhances chemosensitivity

Address correspondence to: Prof. Dr. Ai-Xi Yu, Department of Orthopedics, Zhongnan Hospital of Wuhan University, Wuhan, Hubei 430071, China; Email: yuaixi@whu.edu.cn; or Prof. Ai-Ming Yu, Department of Biochemistry & Molecular Medicine, UC Davis School of Medicine, Sacramento, CA 95817, USA; Email: aimyu@ucdavis.edu.

Number of Text Pages: 24

Number of Figures: 6

Number of References: 45

Number of Words in Abstract: 217

Number of Words in Introduction: 855

Number of Words in Discussion: 1099

Abbreviations: NRF2, nuclear factor (erythroid-derived 2)-like 2; RNAi, RNA interference; siRNA, small interfering RNA; miR or miRNA, microRNA; BERA, bioengineered RNAi agents; OS, osteosarcoma; MSA, sephadex aptamer-tagged methionyl-tRNA; shRNA, short hairpin RNA; ncRNA, noncoding RNA; FPLC, fast protein liquid chromatography; HO-1, heme oxygenase-1; NQO1, NAD(P)H:quinone oxidoreductase 1; ABC transporters, ATP-binding cassette transporters; ROS, reactive oxygen species; HPLC, high performance liquid chromatography; RT-qPCR, reverse transcription quantitative real-time PCR.

Abstract

The nuclear factor (erythroid-derived 2)-like 2 (NRF2) is a transcription factor in the regulation of many oxidative enzymes and efflux transporters critical for oxidative stress and cellular defense against xenobiotics. NRF2 is dysregulated in patient osteosarcoma (OS) tissues and correlates with therapeutic outcomes. Nevertheless, research on the NRF2 regulatory pathways and its potential as a therapeutic target is limited to the use of synthetic small interfering RNA (siRNA) carrying extensive artificial modifications. Herein we report successful high-level expression of recombinant siRNA against NRF2 in *E. coli* using our newly established noncoding RNA bioengineering technology, which was purified to >99% homogeneity using an anion exchange fast protein liquid chromatography method. Bioengineered NRF2-siRNA was able to significantly knock down NRF2 mRNA and protein levels in human OS 143B and MG63 cells, and subsequently suppressed the expression of NRF2-regulated oxidative enzymes (heme oxygenase-1 and NAD(P)H:quinone oxidoreductase 1) and elevated intracellular levels of reactive oxygen species. In addition, recombinant NRF2-siRNA was effective to sensitize both 143B and MG63 cells to doxorubicin, cisplatin and sorafenib, which was associated with significant downregulation of NRF2-targeted ATP-binding cassette (ABC) efflux transporters (ABCC3, ABCC4 and ABCG2). These findings support that targeting NRF2 signaling pathways may improve the sensitivity of cancer cells to chemotherapy, and bioengineered siRNA molecules should be addition to current tools for related research.

Introduction

The nuclear factor (erythroid-derived 2)-like 2 (NRF2 or NFE2L2) is a transcription factor that plays a pivotal role in cellular defense against oxidative and electrophilic stressors or xenobiotics via the induction of a number of oxidative (e.g., heme oxygenase-1 (HO-1) and NAD(P)H:quinone oxidoreductase 1 (NQO1)) and conjugating enzymes (e.g., glutathione S-transferases (GSTs)), as well as efflux ATP-binding cassette (ABC) transporters (e.g., ABCC4 and ABCG2) (see review (Furfaro et al., 2016)). Therefore, activation of NRF2 is traditionally considered as a chemopreventive pathway in xenobiotic metabolism and disposition, and NRF2 has been regarded as a tumor suppressor in cancer research fields. However, there is accumulating evidence that NRF2 may be over-activated in cancer cells, which creates an environment for promoting the survival of cancer cells and conferring resistance to chemotherapy (Jaramillo and Zhang, 2013; Huang et al., 2015; Furfaro et al., 2016). Therefore, more studies are expected to advance our understanding of NRF2 regulatory pathways in cancer cells towards improved cancer therapies.

Osteosarcoma (OS) is the most common primary sarcoma of bone among children, adolescents and young adults (Rivera-Valentin et al., 2015). Anatomically, OS is localized mainly in femur (40%), tibia (20%), and humerus (10%). A major strategy for the treatment of OS patients is the use of neoadjuvant chemotherapy and subsequently extensive resection of tumor tissues followed by further adjuvant chemotherapy for high-grade lesions, which

includes high doses of methotrexate, doxorubicin, and cisplatin (sometimes with ifosfamide) (Jaffe, 2009; Kansara et al., 2014). While this regimen helps OS patients avoid amputation and may dramatically improve overall survival, the 5-year survival rate is around 70%. Moreover, OS exhibits a predilection for pulmonary metastases, and the 5-year survival rate for OS patients with lung metastases drops sharply to 18-33% (Luetke et al., 2014). Therefore, there is a clear need for the development of new therapeutic strategies to fight against malignant OS.

The potential roles of NRF2 in human OS cells have been demonstrated by some studies. First, there is an increased expression of NRF2 among OS patient specimens that is associated with poor clinical outcome and disease-free survival (Park et al., 2012; Zhang et al., 2016). Second, NRF2 expression levels are higher in human OS cells following α -radiation, which may be attenuated by shRNA-mediated gene silencing towards a higher sensitivity to radiation (Chen et al., 2017). On the other hand, lower protein levels of NRF2 and its target HO-1 are accompanied with the increased sensitivity of OS cells to γ -irradiation after the interference of DNA-dependent protein kinase catalytic subunit (DNA-PKcs) (Tang et al., 2014). Furthermore, pharmacological and genetic interference of the pro-survival p38 MAPK/AKT/NRF2/EGR1/HO-1 axis sensitizes OS cells to 15-deoxy- Δ -12,14-prostaglandin J2-mediated apoptosis (Koyani et al., 2016).

While NRF2 represents a promising therapeutic target for the treatment of cancer, current RNA interference (RNAi) materials are limited to synthetic small interfering RNAs (siRNAs) or short hairpin RNA (shRNA)-expressing agents (Singh et al., 2008; Fourtounis et al., 2012; Lu et al., 2016), besides small-molecule modulators that might not be very potent or selective (Sun et al., 2017). Utilization of shRNA-expressing agents (e.g., viral or non-viral vector-based systems) may complicate RNAi processes because they are literally DNA materials that not only rely on the efficiency of gene delivery but also the capacity of host cells or organisms in transcribing DNA to noncoding RNAs (ncRNAs) before the execution of siRNA actions. Furthermore, chemically-engineered siRNAs are comprised of excessive artificial modifications that may exhibit distinct structures, physiochemical properties, biological activities, and safety profiles from natural RNAs produced in cells. Therefore, we have recently developed a novel ncRNA bioengineering technology for the production of natural RNAi agents (e.g., miRNAs and siRNAs) (Li et al., 2014; Chen et al., 2015; Li et al., 2015; Wang et al., 2015). In particular, the tRNA/pre-miR-34a is a robust and versatile carrier to accommodate target small RNAs (Figure 1A) and offers high-level expression of recombinant ncRNAs (Chen et al., 2015). Folded within cells and without artificial modification, these bioengineered RNAi agents (BERA) may better capture the stability, activity, and safety profiles of natural RNAs and thus represent a new class of RNAi materials for biomedical research (Duan and Yu, 2016; Ho and Yu, 2016).

In this study, we aimed to produce a BERA against NRF2 (BERA/NRF2-siRNA) and to assess the application of bioengineered NRF2-siRNA to interfering NRF2 pathways in human OS cells. Following the successful high-level expression of BERA/NRF2-siRNA molecules in *E. coli* using this novel tRNA/pre-miR-34a-based ncRNA bioengineering approach (Chen et al., 2015), recombinant BERA/NRF2-siRNA was purified to >99% homogeneity by an anion-exchange fast protein liquid chromatography (FPLC) method. We further demonstrated that BERA/NRF2-siRNA was selectively processed to target siRNA in human OS cells and remarkably knocked down NRF2 mRNA and protein levels, as compared to cells treated with vehicle or the scaffold sephadex aptamer-tagged methionyl-tRNA (MSA) that has been demonstrated as a valid control for assessing the actions of BERAs through various RNA sequencing and functional studies (Chen et al., 2015; Li et al., 2015; Wang et al., 2015). In addition, a number of NRF2-regulated oxidative enzymes and efflux ABC transporters were subsequently downregulated in OS cells, leading to higher levels of intracellular reactive oxygen species (ROS) and chemosensitivity.

Materials and Methods

Chemicals and materials. Doxorubicin and sorafenib were purchased from LC Laboratories (Woburn, MA, USA). Cisplatin, protease inhibitor cocktail and Trizol reagent were bought from Sigma-Aldrich (St. Louis, MO, USA). Thiazolyl blue tetrazolium bromide (MTT), dimethyl sulfoxide (DMSO) and Bovine Serum Albumin (BSA) were bought from VWR (Radnor, PA, USA). RPMI 1640 medium, fetal bovine serum (FBS) and 0.05% trypsin-EDTA, RIPA buffer, BCA Protein Assay Kit and Lipofectamine 3000 were purchased from Thermo Fisher Scientific (Waltham, MA, USA). PVDF membrane, blotting-grade blocker and Western ECL Substrate kit were purchased from Bio-Rad (Hercules, CA, USA). Direct-zol RNA miniPrep kit was bought from Zymo Research (Irvine, CA, USA). All other chemicals and organic solvents of analytical grade were purchased from Thermo Fisher Scientific or Sigma-Aldrich.

Expression and FPLC purification of BERA/NRF2-siRNA. The production of BERA/NRF2-siRNA and control MSA was carried out using the ncRNA bioengineering technology as we described recently (Li et al., 2014; Chen et al., 2015; Li et al., 2015). Briefly, a DNA fragment encoding the NRF2-siRNA (5'-UAAUUGUCAACUACUGUCAGUU-3') and complementary sequence was cloned into pBSTNAV linearized by *SacII* and *EagI* (New England Biolabs, Ipswich, MA, USA). Plasmids were amplified in DH5 α strain and confirmed by sequencing analyses (Genscript,

Piscataway, NJ, USA). Recombinant ncRNA was produced in HST08 *E. coli* and verified by denaturing urea (8 M) polyacrylamide (8%) gel electrophoresis (PAGE) analysis of total bacterial RNA isolated by phenol extraction.

Anion exchange FPLC purification of BERA/NRF2-siRNA was conducted on a NGC QUEST 10PLUS FPLC system (Bio-Rad) consisting of a fraction collector (Li et al., 2014; Chen et al., 2015). Following urea-PAGE analysis, FPLC fractions containing pure target RNAs were pooled. Recombinant ncRNAs were precipitated with ethanol, reconstituted with nuclease-free water, desalted and then concentrated with Amicon ultra-0.5 mL centrifugal filters (30 KD; EMD Millipore, Billerica, MA, USA). RNA concentrations were determined with a NanoDrop 2000 Spectrophotometer (Thermo Fisher Scientific), and RNA purity (Figure 1) was further determined by a high performance liquid chromatography (HPLC) assay (Chen et al., 2015; Wang et al., 2015).

Cell culture and transfection. Human OS cell lines 143B (CRL-8303) and MG-63 (CRL-1543) were purchased from the American Type Culture Collection (Manassas, VA, USA) with satisfactory authentication. Cells were maintained in RPMI 1640 medium containing 10% FBS, at 37°C in a humidified atmosphere with 5% carbon dioxide and 95% air. Upon arrival cell lines were immediately expanded and frozen. Cell lines used in experiments were replaced with these cryopreserved stocks after 8-12 passages. The

BERA/NRF2-siRNA and control MSA were transfected into the human OS cells within the logarithmic growth phases by using Lipofectamine 3000 reagent, according to the manufacturer's instructions.

RNA isolation and reverse transcription quantitative real-time PCR (RT-qPCR). Human OS 143B and MG63 cells were treated with 10 nM BERA/NRF2-siRNA or MSA for 48 h. Total RNAs were isolated with Direct-zol RNA MiniPrep kit. cDNA was synthesized from total RNAs using NxGen M-MuLV reverse transcriptase (Lucigen, Middleton, WI, USA), with random hexamers or respective stem-loop primers (Table 1). qPCR analyses were carried out using quantitative RT-PCR Green Supermix (Bio-Rad, CA, USA) and gene-specific primers (Table 1) on a CFX96 Touch real-time PCR system (Bio-Rad, CA, USA), as described previously (Chen et al., 2015; Zhao et al., 2015; Zhao et al., 2016). GAPDH and U6 were used as the internal control for the quantification of mRNA and siRNA levels, respectively. Cells were treated in triplicate and assayed separately. The comparative threshold cycle (Ct) method with the formula $2^{-\Delta\Delta C_t}$ was used to calculate the relative gene expression.

Protein isolation and Western blots. Human OS 143B and MG63 cells were treated with 10 nM BERA/NRF2-siRNA or MSA for 48 h. Proteins were extracted from harvested cells using RIPA lysis buffer supplemented with complete protease inhibitors, and protein concentrations

were determined using the BCA Protein Assay Kit. The whole cell proteins (35 µg/lane) were resolved on a 10% SDS-PAGE gel and transferred to a PVDF membrane. Membranes were incubated in 5% Blotting-Grade Blocker (Bio-Rad; Cat. #170-6404) at room temperature for 2 h, and then with primary antibodies, anti-NRF2 antibody (1:1,000 dilution; Abcam, Cambridge, MA, USA; Cat. #ab62352) or anti-β-actin antibody (1:5,000 dilution; Sigma-Aldrich; Cat. #A5441) overnight at 4°C. The membranes were subsequently incubated with the secondary horse radish peroxidase (HRP) labeled anti-mouse (1:3,000 dilution; Cell Signaling Technology, Danvers, MA, USA; Cat. #7076) or anti-rabbit IgG antibodies (1:10,000 dilution; Jackson ImmunoResearch, West Grove, PA, USA; Cat. #111035003) for 2 h, followed with Clarity Western ECL substrates. Proteins were visualized and acquired with a ChemiDoc MP Imaging System (Bio-Rad) and thus quantified by Image Lab software (Bio-Rad). NRF2 protein levels were normalized to β-actin levels in corresponding samples for comparison.

Reactive oxygen species assay. The intracellular ROS levels were determined using the Fluorometric Intracellular ROS kit (Sigma-Aldrich), according to manufacturer's instructions. Briefly, cells were treated with 10 nM BERA/NRF2-siRNA, MSA or vehicle control for 48 h. Fluorescence intensity was recorded (excitation 520 nm and emission 605 nm) using a SpectraMax microplate reader (Molecular Devices, Sunnyvale, CA USA), and ROS levels were normalized to vehicle control treatment group which was set as 100%.

Cytotoxicity assay, chemosensitivity and dose-response relationship. Cells were seeded in 96-well plate (Corning, NY, USA) at 5×10^3 /well in 200 μ L medium and incubated at 37°C overnight. To determine the cytotoxicity of BERA/NRF2-siRNA, cells were treated with different concentrations (0-40 nM) of BERA/NRF2-siRNA or MSA. To evaluate the impact of BERA/NRF2-siRNA on chemosensitivity, cells were treated with 2 nM and/or BERA/NRF2-siRNA or MSA plus various concentrations of doxorubicin (0-300 nM), cisplatin (0-3,000 nM) or sorafenib (0-3,000 nM). After 48 h, cell viability was determined using MTT assay, as we described previously (Wang et al., 2015; Zhao et al., 2015; Zhao et al., 2016).

Cell viability data were normalized to corresponding vehicle control (0 nM drug), which was set as 100%. An inhibitory, normalized response model with variable slope ($Y = 100/(1 + 10^{((\text{LogIC}_{50}-X) \cdot \text{HillSlope})})$; GraphPad Prism, San Diego, CA, USA) was used to estimate the pharmacodynamic parameters (EC₅₀ and Hill Slope) for the anti-proliferative activities of BERA/NRF2-siRNA and MSA since the ncRNAs at the tested concentrations showed a full inhibition. By contrast, chemosensitivity data were fitted to an inhibitory dose-response model with variable slope ($Y = \text{Bottom} + (\text{Top}-\text{Bottom})/(1 + 10^{((\text{LogIC}_{50}-X) \cdot \text{HillSlope})})$; “Top” was not constrained while “Bottom” was constrained to 0 because a low concentration of BERA/NRF2-siRNA in the absence of chemotherapeutics already inhibited cell

proliferation to certain degrees, and this model offered an acceptable Goodness of fit ($R^2 = 0.80-0.99$).

Statistical analysis. All values were presented as mean \pm SD as experiments were carried out in triplicate independently. Data were analyzed using one-way or two-way ANOVA or Student's t-test (GraphPad Prism), depending upon the numbers of groups and variances. Difference was considered as statistically significant when the probability was less than 0.05 ($P < 0.05$).

Results

Expression of BERA/NRF2-siRNA in *E. coli* and purification to a high homogeneity. To produce recombinant NRF2-siRNA agent in *E. coli*, we utilized the tRNA/pre-miR-34a-based ncRNA bioengineering technology (Chen et al., 2015) where miR-34a duplexes were substituted by target NRF2-siRNA (Figure 1A). The predicted secondary structure of BERA/NRF2-siRNA appeared to maintain the stable pre-miR-34a hairpin structure as well as tRNA D-loop and T-loop structures that are identical to MSA. To evaluate the expression of BERA/NRF2-siRNA in *E. coli*, total RNA was isolated and subjected to urea-PAGE analysis. The appearance of a new strong RNA band at the expected size (Figure 1B) in bacteria transformed with BERA/NRF2-siRNA expression plasmid, as compared to the wild type (WT) bacteria, indicated a successful high-level expression of recombinant BERA/NRF2-siRNA in *E. coli*.

To purify BERA/NRF2-siRNA, total RNAs were isolated from bacteria and separated by an anion exchange FPLC method (Chen et al., 2015; Wang et al., 2015). With real-time UV monitoring, FPLC fractions were collected when the peak of target RNA appeared (Figure 1B). A high degree of homogeneity was verified by urea-PAGE analysis of individual fractions, which were combined and desalted to offer final BERA/NRF2-siRNA products. Further HPLC analysis revealed that the resultant BERA/NRF2-siRNA was highly homogenous (> 99% pure; Figure 1C). Given a high-level expression, we generally obtained

18-25 mg total RNAs from 1 L bacterial culture, which offered 4-6 mg pure BERA/NRF2-siRNA following FPLC purification (equivalent to ~20% yield of recombinant BERA/NRF2-siRNA/total RNAs). Likewise, the control scaffold tRNA MSA for assessing the functions of bioengineered RNAi agents, whose validity has been demonstrated by RNA sequencing studies as well as functional analyses (Li et al., 2014; Chen et al., 2015; Wang et al., 2015), was expressed in *E. coli* and purified to a high degree of homogeneity (99.8% pure; Figure 1C).

BERA/NRF2-siRNA is processed to NRF2-siRNA in human OS cells and effectively knocks down NRF2 levels. To examine if BERA/NRF2-siRNA could be processed to target NRF2-siRNA in human OS 143B and MG63 cells, regular qPCR and stem-loop RT-qPCR were conducted to quantitate NRF2-siRNA precursor and NRF2-siRNA, respectively, in cells treated with recombinant ncRNAs for 48 h. The data showed that NRF2-siRNA precursor and NRF2-siRNA levels were approximately 4-fold and 20-fold higher, respectively, in 143B cells transfected with BERA/NRF2-siRNA than MSA or vehicle control (Figure 2A and 2B). Similarly, BERA/NRF2-siRNA-treated MG63 cells showed 30-fold and 8-fold higher levels of NRF2-siRNA precursor and NRF2-siRNA, respectively, than MSA or vehicle control. These results demonstrated that BERA/NRF2-siRNA was successfully transfected into human OS cells and processed to target NRF2-siRNA.

To determine the impact of bioengineered NRF2-siRNA on NRF2 expression in human OS cells, qPCR and immunoblots were carried out to examine NRF2 mRNA and protein levels with specific primers and antibody, respectively. While low concentrations of MSA (10 nM) showed no or minimal effects on NRF2 mRNA or protein expression, as compared to vehicle control (Figure 2C and 2D), BERA/NRF2-siRNA knocked down NRF2 mRNA levels by approximately 70% and 60% in 143B and MG63 cells, respectively, compared to either MSA or vehicle treatment (Figure 2C). Furthermore, as reported in other types of human carcinoma cell lines (Lau et al., 2013), endogenous NRF2 proteins expressed in human OS cells showed two bands that migrate at around 110 kD instead of the predicted molecular weight of 55-65 kD (Figure 2D). The upper NRF2 bands (~110 kD) in 143B and MG63 cells were almost completely knocked out by BERA/NRF2-siRNA while the lower bands (~95 kD) showed 20-30% suppression, as compared to MSA or vehicle control. When the densities of two bands were combined together, NRF2 proteins levels were reduced by 60% in 143B cells and 70% in MG63 cells, respectively, by BERA/NRF2-siRNA (Figure 2D). These findings indicated that bioengineered NRF2-siRNA was effective to silence NRF2 mRNA and protein expression within human OS cells.

Bioengineered NRF2-siRNA reduces the expression of NRF2-regulated oxidative enzymes in human OS cells and alters intracellular ROS levels. Since NRF2 is a major regulator of genes encoding oxidative enzymes in response to oxidative stress (Furfaro et al.,

2016), we examined the consequent effects of bioengineered NRF2-siRNA on HO-1 and NQO1 gene expression as well as cellular ROS accumulation. As determined by qPCR analyses, silencing NRF2 by BERA/NRF2-siRNA (Figure 2) led to a 50% and 60% downregulation of HO-1 and NQO1 mRNA levels, respectively, in 143B cells (Figure 3A and 3B), compared to either MSA or vehicle treatment. Subsequently, a 25% increase of intracellular ROS levels was identified in 143 cells treated with recombinant NRF2-siRNA, as compared to the same doses of MSA (10 nM) or vehicle controls (Figure 3C). Likewise, ROS levels were significantly higher in BERA/NRF2-siRNA-treated MG63 cells, as a result of the downregulation of HO-1 and NQO1 (Figure 3), supporting the actions of bioengineered NRF2-siRNA on NRF2-controlled ROS detoxification.

Biologic NRF2-siRNA is pharmacologically active to inhibit OS cell proliferation. We further defined the antiproliferative activity of bioengineered NRF2-siRNA following the interference of NRF2 signaling pathway. Our data showed that BERA/NRF2-siRNA reduced the proliferation of both 143B and MG63 cells in a dose-dependent manner, and most importantly to a significantly greater degree than MSA control ($P < 0.001$, two-way ANOVA) (Figure 4A), despite that high doses of MSA was also able to inhibit cell proliferation (Li et al., 2015; Wang et al., 2015). The effectiveness of BERA/NRF2-siRNA in suppressing human OS 143B and MG63 cell growth was further manifested by the calculated EC50 values, which were much lower than MSA control (Figure 4B). Together, these findings revealed that

bioengineered NRF2-siRNA was biologically or pharmacologically active in the modulation of OS cell survival, which may be at least partially attributable to the perturbation of NRF2-regulated ROS signaling (Figure 3).

Bioengineered NRF2-siRNA modulates the expression of NRF2-regulated ABC transporters in human OS cells. Recent studies have also demonstrated the role of NRF2 in the regulation of efflux ABC transporters (Adachi et al., 2007; Aleksunes et al., 2008; Malhotra et al., 2010; Singh et al., 2010; Chorley et al., 2012; Canet et al., 2015; Francois et al., 2017). Therefore, we assessed the influence of BERA/NRF2-siRNA on the mRNA levels of five ABC transporters, ABCC1-4/MRP1-4 and ABCG2/BCRP, in human OS cells. Our data showed that, compared to vehicle control, 10 nM MSA did not alter the expression of ABC transporters examined (Figure 5). Interestingly, only ABCC3 mRNA levels were significantly reduced by BERA/NRF2-siRNA in 143B cells by approximately 55%, as compared to either MSA or vehicle treatment, whereas other ABC transporters were not altered (Figure 5A). By contrast, BERA/NRF2-siRNA suppressed ABCC4 and ABCG2 levels by 30% and 25%, respectively, in MG63 cells, compared to MSA or vehicle controls (Figure 5B). These results indicated that recombinant NRF2-siRNA could selectively modulate the expression of particular ABC transporters in human OS cells.

Recombinant NRF2-siRNA molecule is effective to enhance the sensitivity of human OS

cells to doxorubicin, cisplatin and sorafenib. Given the important role of NRF2 in chemosensitivity of cancer cells (Kim et al., 2008; Xu et al., 2014; Li et al., 2017), we defined how interfering NRF2 with biologic siRNA molecule would affect the chemosensitivity of human OS cells. The results showed that a small dose (2 nM) of BERA/NRF2-siRNA significantly ($P < 0.001$, two-way ANOVA) enhanced the sensitivity of both 143B and MG63 cells to doxorubicin, cisplatin and sorafenib, as compared to MSA control (Figure 6A-C). The improved chemosensitivity was further demonstrated by the lower EC50 and “Top” values in BERA/NRF2-siRNA-treated cells than corresponding controls (Figure 6D). Together, these findings indicated that the interference of NRF2 pathways with biologic siRNA molecule could enhance the efficacy of doxorubicin, cisplatin and sorafenib against OS cells.

Discussion

Understanding the functions of transcription factor NRF2 in the regulation of target gene expression and its potential as a therapeutic target depends upon the utilization of proper genetic (Singh et al., 2008; Fourtounis et al., 2012; Lu et al., 2016) and pharmacological (Sun et al., 2017) tools. Distinguished from synthetic siRNA molecules bearing extensive and a wide array of artificial modifications, which vary from different manufacturers and thus pose distinct structures, physicochemical properties, and biological/pharmacological activities, the new recombinant siRNA agent produced in the present study using a novel tRNA/pre-miR-34a-based ncRNA bioengineering technology (Chen et al., 2015) should better capture the properties of natural RNA molecules. Further comprehensive studies demonstrated a selective knockdown of NRF2 mRNA and protein levels within human OS 143B and MG63 cells, following the production of target NRF2-siRNA from BERA/NRF2-siRNA. This led to the interference of NRF2 signaling pathways, as manifested by remarkable changes of NRF2-regulated antioxidant enzymes and efflux transporters. Consequently, bioengineered NRF2-siRNA was effective to modulate intracellular ROS levels and sensitize OS cells to doxorubicin, cisplatin and sorafenib.

NRF2 has been traditionally considered as a critical factor for cell defense and survival, given the fact that NRF2 governs the expression of many detoxification and antioxidant enzymes (Furfaro et al., 2016). Indeed NRF2 is sequestered by Kelch-like ECH-associated protein 1

(KEAP1) in cytoplasm under normal physiological conditions. In response to endogenous and exogenous oxidative or electrophilic stress, NRF2 escapes from KEAP1 suppression, activates its target gene expression after being translocated into the nucleus, and consequently provides chemoprotection. However, NRF2-mediated cytoprotective mechanism is reprogrammed and magnified in a variety of cancer cells. Furthermore, activation of NRF2 facilitates tumor progression and enhances multidrug resistance of cancer cells (Jaramillo and Zhang, 2013; Huang et al., 2015; Furfaro et al., 2016). Therefore, a more complete understanding of NRF2 regulatory pathways in cancer cells is necessary and our bioengineered NRF2-siRNA molecule, whose actions have been demonstrated in the current study, may be a valuable addition to existing tools to interfere NRF2 pathway towards improved understandings.

NRF2 is indeed dysregulated in various types of tumors including OS. One study (Park et al., 2012) revealed that NRF2 is positively expressed in many clinical OS specimens, which forecasts a poor prognostic outcome and correlates with worse disease-free survival. Similarly, another study (Zhang et al., 2016) identified an 8-fold higher nuclear expression rates for NRF2 in OS tissues than normal peritumoral bone tissues, and positive NRF2 expression in OS patients is associated with a significantly lower 5-year survival rate. By contrast, the expression rate of KEAP1, the repressive partner of NRF2, is around 7-fold lower in OS tissues than normal peritumor samples; the 5-year survival rate is significantly

higher in OS patients showing positive KEAP1 expression, as compared to those with negative expression (Zhang et al., 2016). In accordance with targeting NRF2 to control cancer (DeNicola et al., 2011), we observed a dose-dependent antiproliferative activity for bioengineered NRF2-siRNA molecule following the interference of NRF2 signaling pathways in OS cells. These findings should provide insight into developing a new strategy to inhibit NRF2 signaling for the treatment of OS.

The HO-1 enzyme is one of the main targets of NRF2 and a major effector of NRF2-dependent cell response to oxidative stress and xenobiotics (Teppner et al., 2016). A concurrent upregulation of NRF2 and HO-1 is obvious in many types of tumors and correlates well with tumor progression, resistance to therapy, and clinical outcomes (Furfaro et al., 2016). Our finding on the reduction of HO-1 and NQO1 levels in both 143B and MG63 cells demonstrated the consequent effects of knocking down NRF2 on NRF2-regulated gene expression by bioengineered NRF2-siRNA. Furthermore, a higher accumulation of intracellular ROS highlighted the impact of interfering NRF2/HO-1 axis on redox homeostasis (DeNicola et al., 2011; Teppner et al., 2016). In addition, the change of cellular ROS levels following the perturbation of NRF2/HO-1 axis should provide at least partial explanation for the antiproliferative activity of bioengineered NRF2-siRNA against OS cells, as well as the improved cell sensitivity to doxorubicin, cisplatin, and sorafenib.

Chemosensitivity of cancer cells also involves efflux ABC transporter-mediated mechanisms (Choi and Yu, 2014). In agreement with the role of NRF2 in drug resistance, NRF2 has been demonstrated to regulate the expression of many ABC transporters including ABCB6, ABCC1-5 and ABCG2, which may differ due to the differences in types of cells with variable levels of expression and/or distinct regulatory pathways (Adachi et al., 2007; Aleksunes et al., 2008; Malhotra et al., 2010; Singh et al., 2010; Xu et al., 2010; Chorley et al., 2012; Canet et al., 2015; Jeong et al., 2015; Francois et al., 2017). Through interfering NRF2 with bioengineered NRF siRNA, the present study revealed a consequent reduction of ABCC3 expression in 143B cells as well as the suppression of ABCC4 and ABCG2 in MG63 cells, supporting the role of NRF2 in the regulation of ABC transporter expression. Our findings also agree with previous findings on possible differences in the regulation of distinct ABC transporters in different cells lines. For example, ABCC4 levels are significantly upregulated in HepG2 cells and human hepatocytes after the activation of NRF2 (Xu et al., 2010), while ABCG2 levels are readily reduced in lung and prostate cancer cells after knocking down of NRF2 (Singh et al., 2010). In addition, consistent with previous findings on an increased chemosensitivity for lung cancer cells after the disruption of NRF2-ABCG2 cascade (Singh et al., 2010), treatment with bioengineered NRF2-siRNA sensitized OS cells to doxorubicin, cisplatin and sorafenib. Given the facts that doxorubicin and sorafenib are substrates of ABC transporters (Miyake et al., 1999; Zhou et al., 2001; Lagas et al., 2010; Agarwal et al., 2011) and cisplatin efficacy is highly related to ABCC2 expression (see review (Baiceanu et al.,

2015)), the suppression of ABC transporter expression may offer further explanations for the enhanced chemosensitivity, besides the direct antiproliferative activity of NRF-siRNA.

In summary, we have demonstrated a successful high-level production of a novel biologic NRF2-siRNA agent using our newly established ncRNA bioengineering technology. The bioengineered NRF2-siRNA molecule was effective to silence NRF2 expression in human cancer cells, which consequently reduced the expression of NRF2-regulated oxidative enzymes and led to higher intracellular ROS levels. In addition, knocking down NRF2 with bioengineered siRNA agent improved chemosensitivity of cancer cells, which was associated with the suppression of NRF2-regulated efflux ABC transporters. These findings not only support the intervention of NRF2 signaling pathways as a new therapeutic strategy to combat cancer but also point to promising new direction for the development and use of biologic RNAi agents for drug disposition research as well as broad basic and translational studies.

Authorship Contributions

Participated in research design: Yu, Li, and all other authors.

Conducted experiments: Li, Tu, Ho, Jilek, Duan and Zhang.

Contributed to new reagents or analytical tools: A.-M. Yu and A.-X. Yu.

Performed data analysis: Li, Yu and all other authors.

Wrote or contributed to the writing of the manuscript: Yu, Li, and all other authors.

References

- Adachi, T., H. Nakagawa, I. Chung, Y. Hagiya, K. Hoshijima, N. Noguchi, M. T. Kuo and T. Ishikawa (2007). Nrf2-dependent and -independent induction of ABC transporters ABCC1, ABCC2, and ABCG2 in HepG2 cells under oxidative stress. *J Exp Ther Oncol* **6**: 335-348.
- Agarwal, S., R. Sane, J. R. Ohlfest and W. F. Elmquist (2011). The role of the breast cancer resistance protein (ABCG2) in the distribution of sorafenib to the brain. *J Pharmacol Exp Ther* **336**: 223-233.
- Aleksunes, L. M., A. L. Slitt, J. M. Maher, L. M. Augustine, M. J. Goedken, J. Y. Chan, N. J. Cherrington, C. D. Klaassen and J. E. Manautou (2008). Induction of Mrp3 and Mrp4 transporters during acetaminophen hepatotoxicity is dependent on Nrf2. *Toxicol Appl Pharmacol* **226**: 74-83.
- Baiceanu, E., G. Crisan, F. Loghin and P. Falson (2015). Modulators of the human ABCC2: hope from natural sources? *Future Med Chem* **7**: 2041-2063.
- Canet, M. J., M. D. Merrell, B. G. Harder, J. M. Maher, T. Wu, A. J. Lickteig, J. P. Jackson, D. D. Zhang, M. Yamamoto and N. J. Cherrington (2015). Identification of a functional antioxidant response element within the eighth intron of the human ABCC3 gene. *Drug Metab Dispos* **43**: 93-99.
- Chen, N., R. Zhang, T. Konishi and J. Wang (2017). Upregulation of NRF2 through autophagy/ERK 1/2 ameliorates ionizing radiation induced cell death of human osteosarcoma U-2 OS. *Mutat Res* **813**: 10-17.
- Chen, Q. X., W. P. Wang, S. Zeng, S. Urayama and A. M. Yu (2015). A general approach to high-yield biosynthesis of chimeric RNAs bearing various types of functional small RNAs for broad applications. *Nucleic Acids Res* **43**: 3857-3869.
- Choi, Y. H. and A. M. Yu (2014). ABC transporters in multidrug resistance and pharmacokinetics, and strategies for drug development. *Curr Pharm Des* **20**: 793-807.
- Chorley, B. N., M. R. Campbell, X. Wang, M. Karaca, D. Sambandan, F. Bangura, P. Xue, J. Pi, S. R. Kleeberger and D. A. Bell (2012). Identification of novel NRF2-regulated genes by ChIP-Seq: influence on retinoid X receptor alpha. *Nucleic Acids Res* **40**: 7416-7429.
- DeNicola, G. M., F. A. Karreth, T. J. Humpton, A. Gopinathan, C. Wei, K. Frese, D. Mangal, K. H. Yu, C. J. Yeo, E. S. Calhoun, F. Scrimieri, J. M. Winter, R. H. Hruban, C. Iacobuzio-Donahue, S. E. Kern, I. A. Blair and D. A. Tuveson (2011). Oncogene-induced Nrf2 transcription promotes ROS detoxification and tumorigenesis. *Nature* **475**: 106-109.

- Duan, Z. and A. M. Yu (2016). Bioengineered non-coding RNA agent (BERA) in action. *Bioengineered*: 1-7.
- Fourtounis, J., I. M. Wang, M. C. Mathieu, D. Claveau, T. Loo, A. L. Jackson, M. A. Peters, A. G. Therien, Y. Boie and M. A. Crackower (2012). Gene expression profiling following NRF2 and KEAP1 siRNA knockdown in human lung fibroblasts identifies CCL11/Eotaxin-1 as a novel NRF2 regulated gene. *Respir Res* **13**: 92.
- Francois, L. N., L. Gorczyca, J. Du, K. M. Bircsak, E. Yen, X. Wen, M. J. Tu, A. M. Yu, N. P. Illsley, S. Zamudio and L. M. Aleksunes (2017). Down-regulation of the placental BCRP/ABCG2 transporter in response to hypoxia signaling. *Placenta* **51**: 57-63.
- Furfaro, A. L., N. Traverso, C. Domenicotti, S. Piras, L. Moretta, U. M. Marinari, M. A. Pronzato and M. Nitti (2016). The Nrf2/HO-1 Axis in Cancer Cell Growth and Chemoresistance. *Oxid Med Cell Longev* **2016**: 1958174.
- Ho, P. Y. and A. M. Yu (2016). Bioengineering of noncoding RNAs for research agents and therapeutics. *Wiley Interdiscip Rev RNA* **7**: 186-197.
- Huang, Y., W. Li, Z. Y. Su and A. N. Kong (2015). The complexity of the Nrf2 pathway: beyond the antioxidant response. *J Nutr Biochem* **26**: 1401-1413.
- Jaffe, N. (2009). Osteosarcoma: review of the past, impact on the future. The American experience. *Cancer Treat Res* **152**: 239-262.
- Jaramillo, M. C. and D. D. Zhang (2013). The emerging role of the Nrf2-Keap1 signaling pathway in cancer. *Genes Dev* **27**: 2179-2191.
- Jeong, H. S., I. G. Ryoo and M. K. Kwak (2015). Regulation of the expression of renal drug transporters in KEAP1-knockdown human tubular cells. *Toxicol In Vitro* **29**: 884-892.
- Kansara, M., M. W. Teng, M. J. Smyth and D. M. Thomas (2014). Translational biology of osteosarcoma. *Nat Rev Cancer* **14**: 722-735.
- Kim, H. R., S. Kim, E. J. Kim, J. H. Park, S. H. Yang, E. T. Jeong, C. Park, M. J. Youn, H. S. So and R. Park (2008). Suppression of Nrf2-driven heme oxygenase-1 enhances the chemosensitivity of lung cancer A549 cells toward cisplatin. *Lung Cancer* **60**: 47-56.
- Koyani, C. N., K. Kitz, C. Rossmann, E. Bernhart, E. Huber, C. Trummer, W. Windischhofer, W. Sattler and E. Malle (2016). Activation of the MAPK/Akt/Nrf2-Egr1/HO-1-GCLc axis protects MG-63 osteosarcoma cells against 15d-PGJ2-mediated cell death. *Biochem Pharmacol* **104**: 29-41.

Lagas, J. S., R. A. van Waterschoot, R. W. Sparidans, E. Wagenaar, J. H. Beijnen and A. H. Schinkel (2010). Breast cancer resistance protein and P-glycoprotein limit sorafenib brain accumulation. *Mol Cancer Ther* **9**: 319-326.

Lau, A., W. Tian, S. A. Whitman and D. D. Zhang (2013). The predicted molecular weight of Nrf2: it is what it is not. *Antioxid Redox Signal* **18**: 91-93.

Li, K., L. Ouyang, M. He, M. Luo, W. Cai, Y. Tu, R. Pi and A. Liu (2017). IDH1 R132H mutation regulates glioma chemosensitivity through Nrf2 pathway. *Oncotarget* **8**: 28865-28879.

Li, M. M., B. Addepalli, M. J. Tu, Q. X. Chen, W. P. Wang, P. A. Limbach, J. M. LaSalle, S. Zeng, M. Huang and A. M. Yu (2015). Chimeric MicroRNA-1291 Biosynthesized Efficiently in Escherichia coli Is Effective to Reduce Target Gene Expression in Human Carcinoma Cells and Improve Chemosensitivity. *Drug Metab Dispos* **43**: 1129-1136.

Li, M. M., W. P. Wang, W. J. Wu, M. Huang and A. M. Yu (2014). Rapid Production of Novel Pre-MicroRNA Agent hsa-mir-27b in Escherichia coli Using Recombinant RNA Technology for Functional Studies in Mammalian Cells. *Drug Metab Dispos* **42**: 1791-1795.

Lu, C., W. Xu, F. Zhang, J. Shao and S. Zheng (2016). Nrf2 knockdown attenuates the ameliorative effects of ligustrazine on hepatic fibrosis by targeting hepatic stellate cell transdifferentiation. *Toxicology* **365**: 35-47.

Luetke, A., P. A. Meyers, I. Lewis and H. Juergens (2014). Osteosarcoma treatment - where do we stand? A state of the art review. *Cancer Treat Rev* **40**: 523-532.

Malhotra, D., E. Portales-Casamar, A. Singh, S. Srivastava, D. Arenillas, C. Happel, C. Shyr, N. Wakabayashi, T. W. Kensler, W. W. Wasserman and S. Biswal (2010). Global mapping of binding sites for Nrf2 identifies novel targets in cell survival response through ChIP-Seq profiling and network analysis. *Nucleic Acids Res* **38**: 5718-5734.

Miyake, K., L. Mickley, T. Litman, Z. Zhan, R. Robey, B. Cristensen, M. Brangi, L. Greenberger, M. Dean, T. Fojo and S. E. Bates (1999). Molecular cloning of cDNAs which are highly overexpressed in mitoxantrone-resistant cells: demonstration of homology to ABC transport genes. *Cancer Res* **59**: 8-13.

Park, J. Y., Y. W. Kim and Y. K. Park (2012). Nrf2 expression is associated with poor outcome in osteosarcoma. *Pathology* **44**: 617-621.

Rivera-Valentin, R. K., L. Zhu and D. P. Hughes (2015). Bone Sarcomas in Pediatrics: Progress in Our Understanding of Tumor Biology and Implications for Therapy. *Paediatr Drugs* **17**: 257-271.

Singh, A., S. Boldin-Adamsky, R. K. Thimmulappa, S. K. Rath, H. Ashush, J. Coulter, A. Blackford, S. N. Goodman, F. Bunz, W. H. Watson, E. Gabrielson, E. Feinstein and S. Biswal (2008). RNAi-mediated silencing of nuclear factor erythroid-2-related factor 2 gene expression in non-small cell lung cancer inhibits tumor growth and increases efficacy of chemotherapy. *Cancer Res* **68**: 7975-7984.

Singh, A., H. Wu, P. Zhang, C. Happel, J. Ma and S. Biswal (2010). Expression of ABCG2 (BCRP) is regulated by Nrf2 in cancer cells that confers side population and chemoresistance phenotype. *Mol Cancer Ther* **9**: 2365-2376.

Sun, H., J. Zhu, H. Lin, K. Gu and F. Feng (2017). Recent progress in the development of small molecule Nrf2 modulators: a patent review (2012-2016). *Expert Opin Ther Pat* **27**: 763-785.

Tang, X., F. Yuan and K. Guo (2014). Repair of radiation damage of U2OS osteosarcoma cells is related to DNA-dependent protein kinase catalytic subunit (DNA-PKcs) activity. *Mol Cell Biochem* **390**: 51-59.

Teppner, M., F. Boess, B. Ernst and A. Pahler (2016). Biomarkers of Flutamide-Bioactivation and Oxidative Stress In Vitro and In Vivo. *Drug Metab Dispos* **44**: 560-569.

Wang, W. P., P. Y. Ho, Q. X. Chen, B. Addepalli, P. A. Limbach, M. M. Li, W. J. Wu, J. L. Jilek, J. X. Qiu, H. J. Zhang, T. Li, T. Wun, R. D. White, K. S. Lam and A. M. Yu (2015). Bioengineering Novel Chimeric microRNA-34a for Prodrug Cancer Therapy: High-Yield Expression and Purification, and Structural and Functional Characterization. *J Pharmacol Exp Ther* **354**: 131-141.

Xu, S., J. Weerachayaphorn, S. Y. Cai, C. J. Soroka and J. L. Boyer (2010). Aryl hydrocarbon receptor and NF-E2-related factor 2 are key regulators of human MRP4 expression. *Am J Physiol Gastrointest Liver Physiol* **299**: G126-135.

Xu, X., Y. Zhang, W. Li, H. Miao, H. Zhang, Y. Zhou, Z. Li, Q. You, L. Zhao and Q. Guo (2014). Wogonin reverses multi-drug resistance of human myelogenous leukemia K562/A02 cells via downregulation of MRP1 expression by inhibiting Nrf2/ARE signaling pathway. *Biochem Pharmacol* **92**: 220-234.

Zhang, J., X. Wang, W. Wu, H. Dang and B. Wang (2016). Expression of the Nrf2 and Keap1 proteins and their clinical significance in osteosarcoma. *Biochem Biophys Res Commun* **473**: 42-46.

Zhao, Y., M. J. Tu, W. P. Wang, J. X. Qiu, A. X. Yu and A. M. Yu (2016). Genetically engineered pre-microRNA-34a prodrug suppresses orthotopic osteosarcoma xenograft tumor

growth via the induction of apoptosis and cell cycle arrest. *Sci Rep* **6**: 26611.

Zhao, Y., M. J. Tu, Y. F. Yu, W. P. Wang, Q. X. Chen, J. X. Qiu, A. X. Yu and A. M. Yu (2015). Combination therapy with bioengineered miR-34a prodrug and doxorubicin synergistically suppresses osteosarcoma growth. *Biochem Pharmacol* **98**: 602-613.

Zhou, S., J. D. Schuetz, K. D. Bunting, A. M. Colapietro, J. Sampath, J. J. Morris, I. Lagutina, G. C. Grosveld, M. Osawa, H. Nakauchi and B. P. Sorrentino (2001). The ABC transporter Bcrp1/ABCG2 is expressed in a wide variety of stem cells and is a molecular determinant of the side-population phenotype. *Nat Med* **7**: 1028-1034.

Footnotes

This work was supported in part by Outstanding Medical Academic leader Program of Hubei Province and Huanghe Yingcai Program of Wuhan (A.X.Y.); the National Institutes of Health [Grants R01GM113888 and U01CA175315 (A.M.Y.)]. P.-C. L. was supported by a Graduate Student Fellowship from the Academic Exchange Program at Wuhan University.

Send reprint requests to: Prof. Ai-Xi Yu, Department of Orthopedics, Zhongnan Hospital of Wuhan University, Wuhan, Hubei 430071, China; Email: yuaixi@whu.edu.cn; or Prof. Ai-Ming Yu, Department of Biochemistry & Molecular Medicine, UC Davis School of Medicine, Sacramento, CA 95817, USA; Email: aimyu@ucdavis.edu.

Legends for Figures

Figure 1. Bioengineering NRF2-siRNA molecule. (A) The secondary structure of bioengineered RNAi molecule against NRF2 (BERA/NRF2-siRNA) was predicted by RNAfold (<http://rna.tbi.univie.ac.at/cgi-bin/RNAWebSuite/RNAfold.cgi>), where the NRF2-siRNA replaced miR-34a duplexes within the tRNA/pre-miR-34a-based carrier. The control tRNA MSA is shown for comparison. The heat color gradation indicates the base-pairing probability from 0 to 1. (B) FPLC trace during the purification of BERA/NRF2-siRNA. The insert shows urea-PAGE analysis of the targeted RNA fractions (#1, 2, 3 and 4). (C) The purity (> 99%) of isolated BERA/NRF2-siRNA and control MSA was confirmed by HPLC analysis.

Figure 2. Biologic BERA/NRF2-siRNA is processed to NRF2-siRNA in human OS cells, and consequently knocked down the NRF2 mRNA and protein expression levels. Human 143B and MG63 cells were transfected with 10 nM BERA/NERF2-siRNA, control MSA or vehicle for 48 h. Levels of NRF2-siRNA precursor (A) and NRF2-siRNA (B) in BERA/NRF2-siRNA treated cells were significantly higher than MSA or vehicle controls. As a result, NRF2 mRNA (C) and protein (D; densities of two bands combined together) levels were significantly reduced in cells by BERA/NRF2-siRNA, compared to either MSA or vehicle treatments that did not differ. Values are mean \pm SD of triplicate treatments. * $P < 0.05$; ** $P < 0.01$; *** $P < 0.001$, compared to vehicle or MSA control group (one-way

ANOVA).

Figure 3. Bioengineered NRF2-siRNA reduces the mRNA levels of NRF2-regulated genes that encode oxidative enzymes, and thus leads to a higher level of intracellular ROS. The mRNA levels of NRF2 target genes HO-1 (A) and NQO1 (B) were decreased significantly by BERA/NRF2-siRNA in 143B and MG63 cells, which resulted in a higher ROS level (C), as compared to either MSA or vehicle treatments. Values are mean \pm SD of triplicate treatments. $*P < 0.05$ and $***P < 0.001$, compared to vehicle or MSA controls (one-way ANOVA).

Figure 4. Bioengineered NRF2-siRNA inhibits human OS cell proliferation. (A) BERA/NRF2-siRNA significantly suppressed the growth of 143B and MG63 cells in a dose-dependent manner and to a greater degree than the control MSA (Values are mean \pm SD of triplicate treatments; two-way ANOVA with Bonferroni post-hoc tests: $p < 0.001$ for drug treatment and dose; $***p < 0.001$, $**p < 0.01$, and $*p < 0.05$ at indicated doses, compared to corresponding MSA control). (B) The estimated EC50 and Hill slope values for the inhibition of human OS cell proliferation by BERA/NRF2-siRNA and control MSA ($***P < 0.001$, compared to the MSA control; Student's t-test).

Figure 5. Bioengineered NRF2-siRNA alters the expression of NRF2-regulated ABC

transporters in human OS 143B and MG63 cells. (A) The mRNA level of MRP3/ABCC3 was decreased significantly by BERA/NRF2-siRNA in 143B cells, compared to MSA or vehicle treatments. (B) The mRNA levels of MRP4/ABCC4 and BCRP/ABCG2 were reduced significantly by BERA/NRF2-siRNA in MG63 cells, as compared to MSA or vehicle controls. Values are mean \pm SD of triplicate treatments. $*P < 0.05$; $**P < 0.01$; $***P < 0.001$, compared to vehicle or MSA treatments (one-way ANOVA).

Figure 6. BERA/NRF2-siRNA improves the chemosensitivity of human OS cells.

BERA/NRF2-siRNA (2 nM) significantly sensitized 143B and MG63 cells to doxorubicin (A), cisplatin (B) and sorafenib (C), respectively (Values are mean \pm SD of triplicate treatments; two-way ANOVA with Bonferroni post-hoc tests: $p < 0.001$ for drug treatment and dose; $***p < 0.001$, and $**p < 0.01$ at indicated doses, compared to the same doses of MSA). (D) The estimated EC50, Hill slope and Top values for doxorubicin, cisplatin and sorafenib cytotoxicity against BERA/NRF2-siRNA- and MSA-treated 143B and MG63 cells ($**P < 0.01$; $***P < 0.001$, compared to MSA control; Student's t-test).

Table 1. The sequences of primers used in the study.

| Gene | | Sequence |
|------------|---------|---|
| U6 | Forward | 5'-CTCGCTTCGGCAGCACA-3' |
| | Reverse | 5'-AACGCTTCACGAATTTGCGT-3' |
| | RT | 5'-GTCGTATCCAGTGCAGGGTCCGAGGTATTCGCACTGGATACGACAACTGAA-3' |
| NRF2-siRNA | Forward | 5'-GGCGCCTAATTGTCAACTTCTG-3' |
| | Reverse | 5'-GTGCAGGGTCCGAGGT-3' |
| BERA/ | Forward | 5'-GGCCAGCTGTGAGTGTTCCTT-3' |
| NRF2-siRNA | Reverse | 5'-GGGCCAACAACGTGCAGC-3' |
| GAPDH | Forward | 5'-ATCACCATCTTCCAGGAGCGA-3' |
| | Reverse | 5'-GCTTCACCACCTTCTTGATGT-3' |
| NRF2 | Forward | 5'-TGAGGTTTCTTCGGCTACGTT-3' |
| | Reverse | 5'-CTTCTGTCAGTTTGGCTTCTGG-3' |
| HO-1 | Forward | 5'-CTGGAGGAGGAGATTGAGCG-3' |
| | Reverse | 5'-ATGGCTGGTGTGTAGGGGAT-3' |
| NQO1 | Forward | 5'- TGCAGCGGCTTTGAAGAAGAAAGG-3' |
| | Reverse | 5'-TCGGCAGGATACTGAAAGTTCGCA-3' |
| ABCC1 | Forward | 5'-AACCTGGACCCATTCAGCC-3' |
| | Reverse | 5'-GACTGGATGAGGTCGTCCGT-3' |
| ABCC2 | Forward | 5'-AGCAGCCATAGAGCTGGCCCT-3' |
| | Reverse | 5'-AGCAAAACCAGGAGCCATGTG-3' |
| ABCC3 | Forward | 5'-CAGAGAAGGTGCAGGTGACA-3' |
| | Reverse | 5'-CTAAAGCAGCATAGACGCCC-3' |
| ABCC4 | Forward | 5'-TGATGAGCCGTATGTTTTGC-3' |
| | Reverse | 5'-CTTCGGAACGGACTTGACAT-3' |
| ABCG2 | Forward | 5'-CAGGTGGAGGCAAATCTTCGT-3' |
| | Reverse | 5'-ACACACCACGGATAAACTGA-3' |

Figure 1

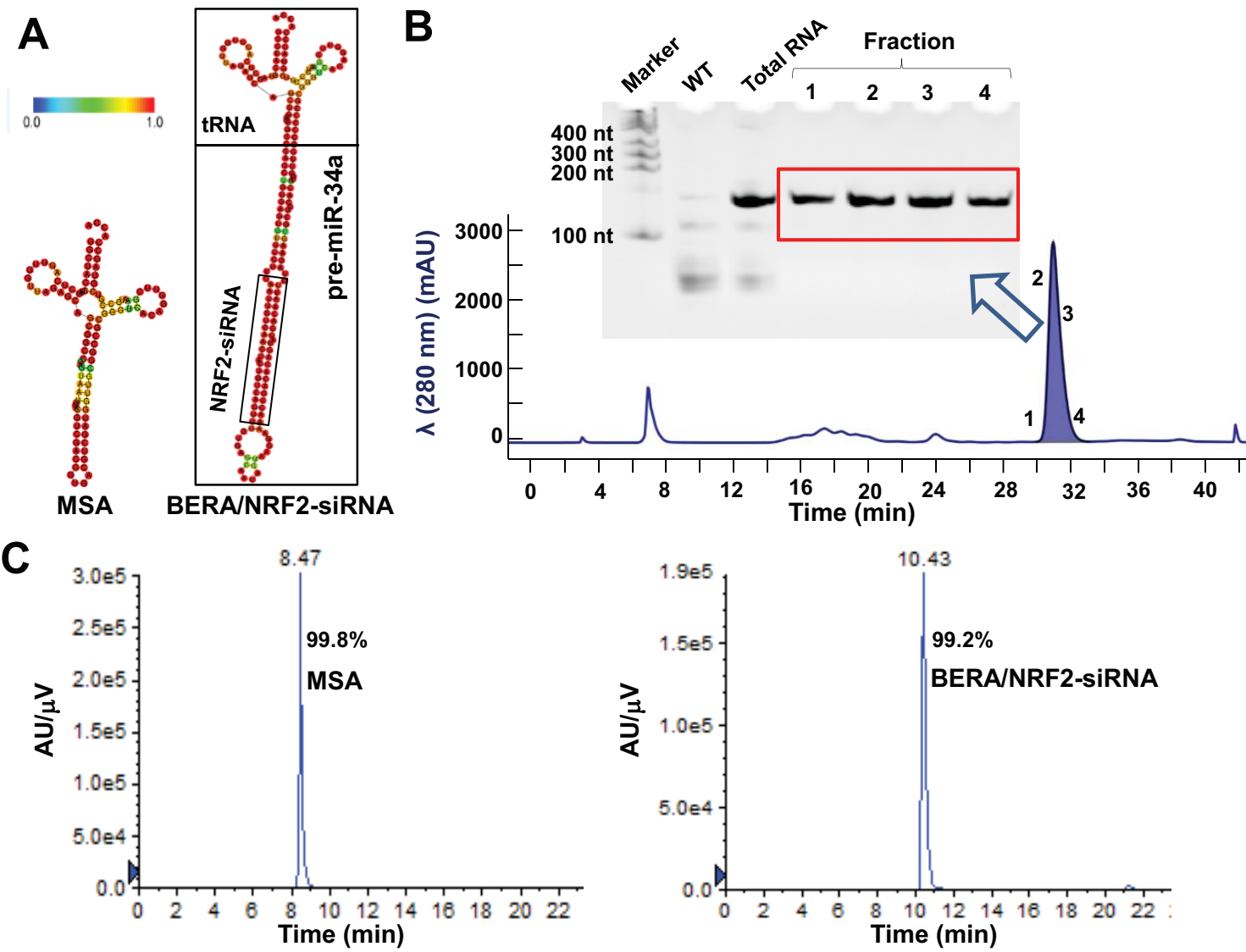


Figure 2

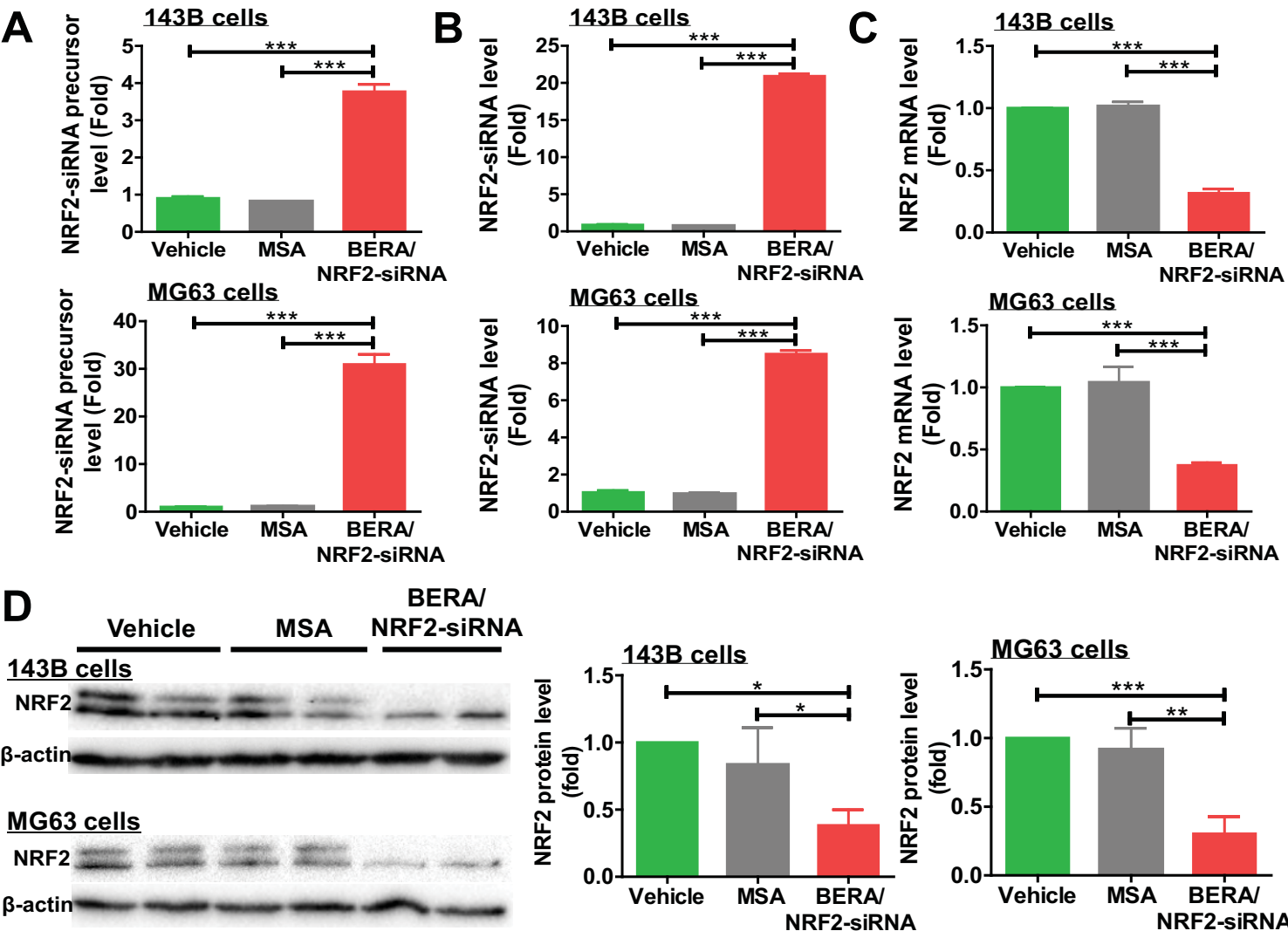


Figure 3

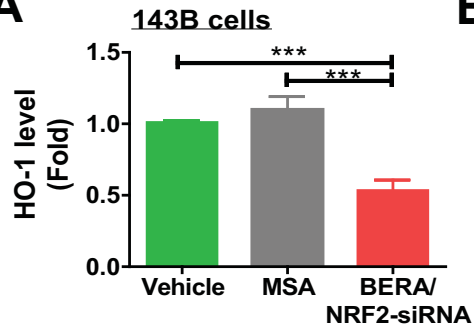
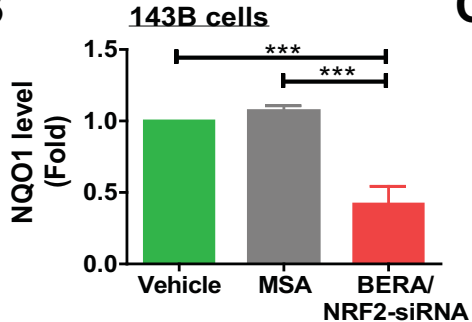
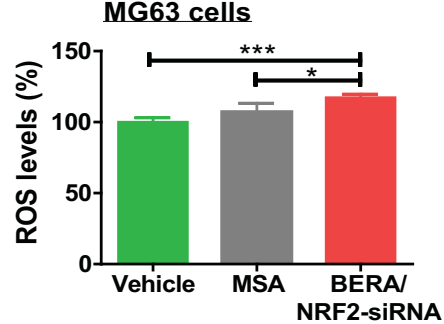
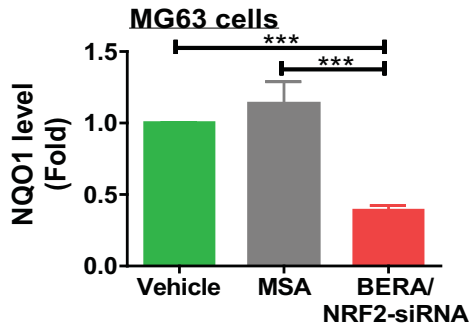
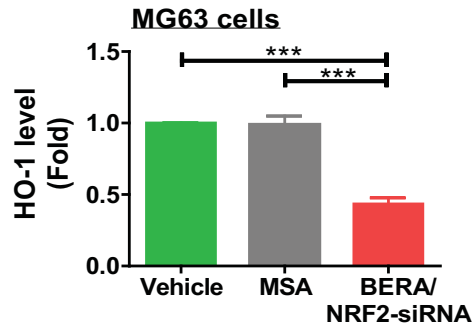
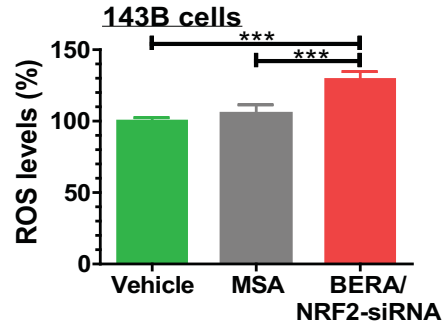
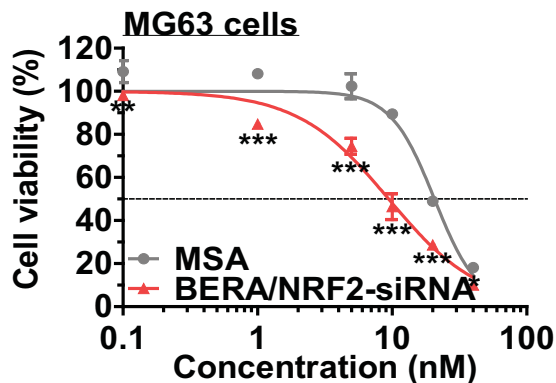
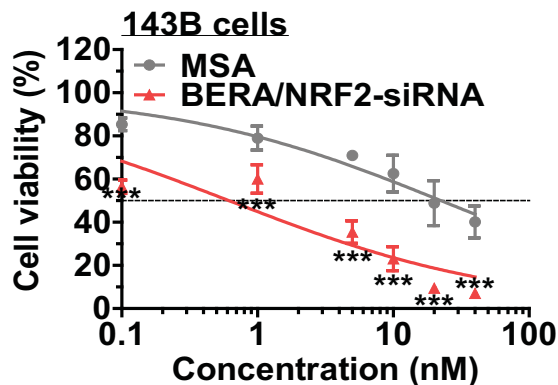
A**B****C**

Figure 4

A



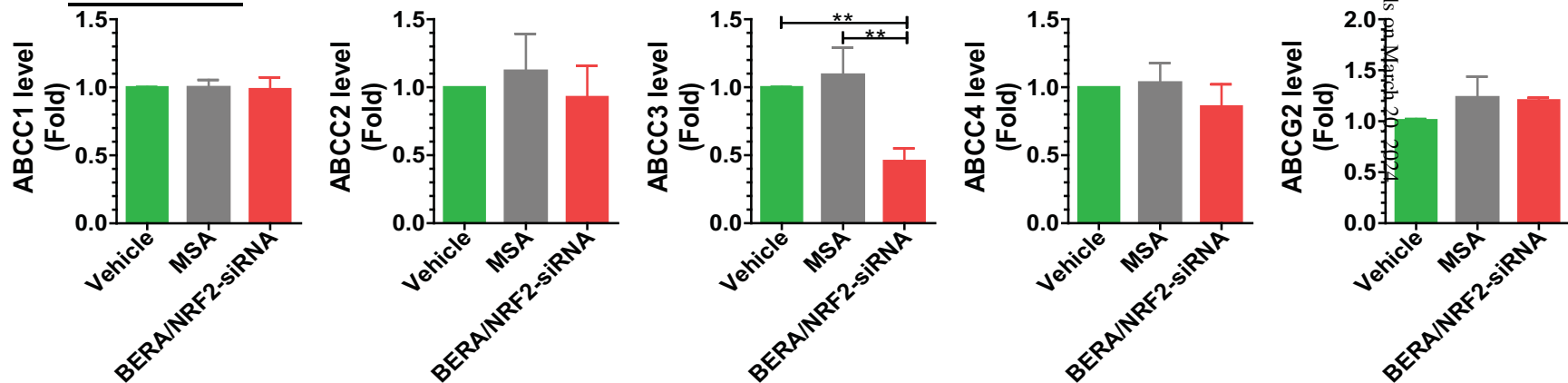
B

| Cell line | EC50 (nM) | | Hill Slope | |
|-----------|--------------|---------------------|--------------|---------------------|
| | MSA | BERA/ NRF2-siRNA | MSA | BERA/ NRF2-siRNA |
| 143B | 22.46 ± 1.21 | 0.62 ± 1.38*** | -0.44 ± 0.06 | -0.42 ± 0.06 |
| MG63 | 20.61 ± 1.05 | 9.42 ± 1.07*** | -2.67 ± 0.33 | -1.28 ± 0.12*** |

Figure 5

A

143B cells



B

MG63 cells

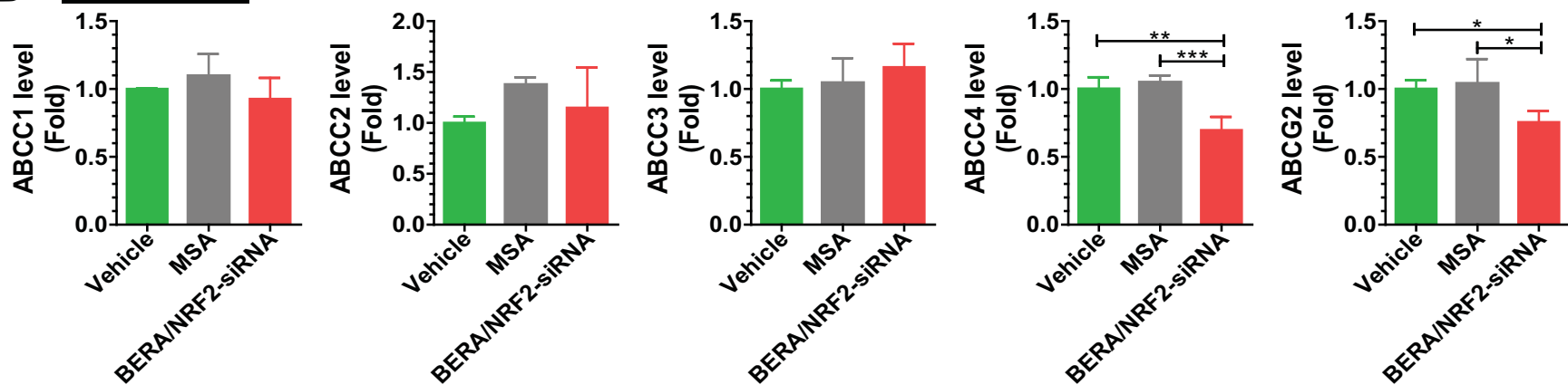
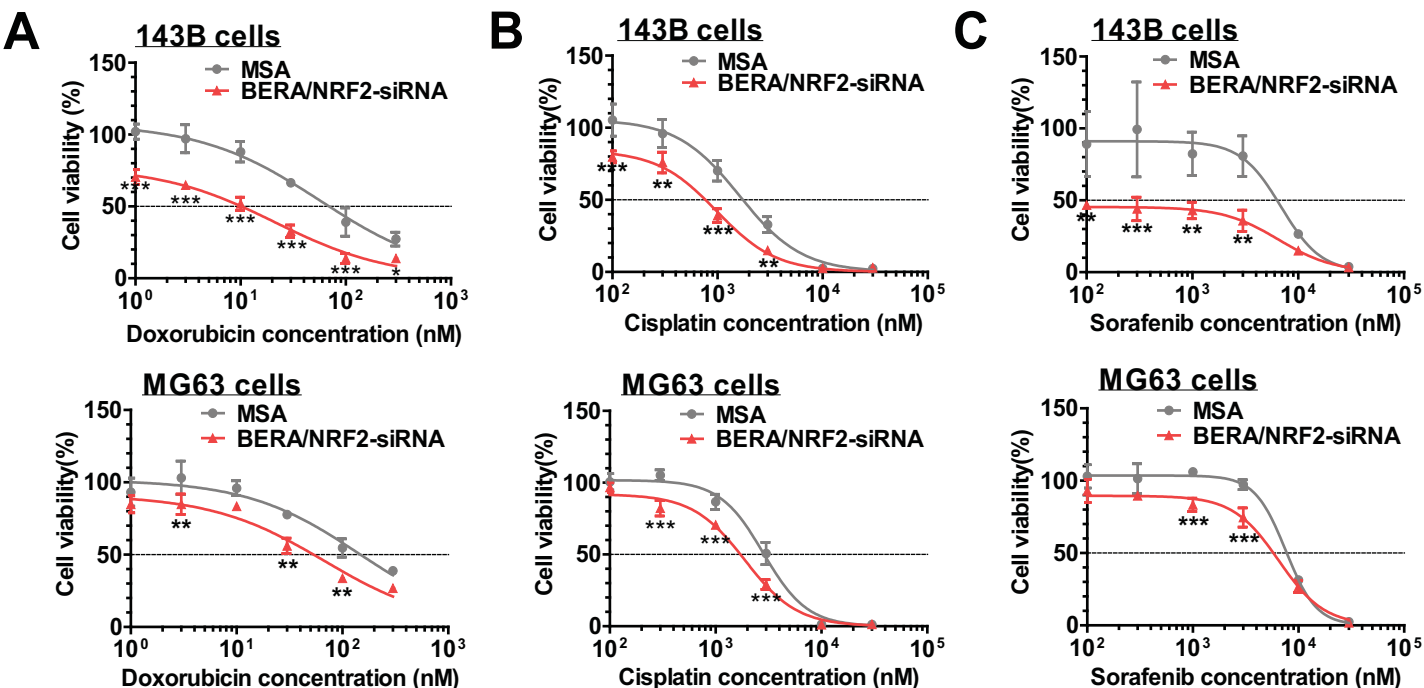


Figure 6



| Drug | Cell line | EC50 (nM) | | Hill Slope | | Top | |
|-------------|-----------|--------------|-----------------|--------------|-----------------|--------------|-----------------|
| | | MSA | BERA/NRF2-siRNA | MSA | BERA/NRF2-siRNA | MSA | BERA/NRF2-siRNA |
| Doxorubicin | 143B | 57.41 ± 1.23 | 21.44 ± 1.27*** | -0.76 ± 0.11 | -0.79 ± 0.11 | 107.8 ± 5.5 | 77.66 ± 4.99*** |
| | MG63 | 142.2 ± 1.2 | 67.59 ± 1.24*** | -0.82 ± 0.16 | -0.81 ± 0.13 | 101.8 ± 4.7 | 91.37 ± 4.77*** |
| Cisplatin | 143B | 1620 ± 1 | 982.8 ± 1.1*** | -1.46 ± 0.20 | -1.53 ± 0.19 | 105.7 ± 4.1 | 84.29 ± 3.29*** |
| | MG63 | 2832 ± 1 | 1894 ± 1*** | -2.10 ± 0.26 | -1.76 ± 0.17*** | 101.7 ± 2.2 | 91.97 ± 2.15*** |
| Sorafenib | 143B | 6882 ± 1 | 6512 ± 1*** | -2.29 ± 0.94 | -1.65 ± 0.32** | 91.07 ± 6.10 | 45.39 ± 1.83*** |
| | MG63 | 7559 ± 1 | 6503 ± 1*** | -2.97 ± 0.49 | -2.01 ± 0.23*** | 103.6 ± 1.8 | 89.56 ± 1.91*** |